Global Journal of Pure and Applied Mathematics.
ISSN 0973-1768 Volume 11, Number 6 (2015), pp. 4923-4935

http://www.ripublication.com/gjpam.htm

Contact problem decision for airframe assembly simulation in case of non-conformal meshes in a junction area

A. Avramenko[1]

Centre of Computational Engineering and Integrated Design (CEID), Lappeenranta University of Technology, Skinnarilankatu 34, 53850, Lappeenranta, Finland.
E-mail: Anna.Avramenko@lut.fi

O. Agafonova

Lappeenranta University of Technology, School of Engineering Science, Skinnarilankatu 34, 53850, Lappeenranta, Finland.
E-mail: Oxana.Agafonova@lut.fi

H. Haario

Lappeenranta University of Technology, School of Engineering Science, Skinnarilankatu 34, 53850, Lappeenranta, Finland.
E-mail: Heikki.Haario@lut.fi

Abstract

This paper is devoted to further development of numerical methods for simulation of fuselage junction riveting process. The methodology of a contact problem solving was developed to simulate the aircraft assembly process. The special algorithm reduces the dimension of the problem after eliminating the unknowns outside the contact zone and the initial problem transforms into the problem of quadratic programming with linear constraints. As the installed fasteners restrict relative tangential displacements of assembled details in the junction area, the relative tangential displacements are negligible in comparison with normal ones. This special

[1]Corresponding author.

feature of the problem justifies implementation of node-to-node contact model that is much simpler than general surface-to-surface model. But it also means that all finite element nodes of details in the contact area should coincide completely. This restriction creates difficulties during mesh building because it is much easier to build meshes of the details independently from each other. This article introduces the method and the modernized algorithm for the riveting process with non-conformal meshes. The algorithm was developed in C++ for two-dimensional membrane cases using the finite element method.

AMS subject classification:
Keywords: Non-conformal meshes, contact problem, riveting process, finite element method, quadratic programming.

1. Introduction

The optimization and acceleration of assembly process is one of the important problems for aircraft building companies. All main parts of the airframe are joined together during the riveting process. The assembly line is very complicated and consists of several stages. It is important to control gap between joined details and stresses caused by installed fasteners during this process. From the one size absolute contact between details should be achieved. From another one engineers should avoid cracks, composite layer separation and detail destruction. Therefore, a special tool was developed which allows engineers to perform simulations in order to evaluate displacements and stresses of aircraft details on the assembly line. This special numerical method is used for solving a class of contact problems that particularly arise during the simulation of riveting process. The concept of basic numerical algorithm as well as validation tests were described in [3,4]. Only the general approach of this method is presented in this paper.

Figure 1 presents finite element model of two details which are fixed at the ends.

The contact between details is possible only inside the junction area that is shown by blue lines. Initially, details are separated by the distance called an initial gap. Let choose a set consisting of n finite element nodes in the junction area $X = (x_1, x_2, \ldots, x_n)$ and call it as computational nodes. This net includes the nodes of upper and lower details, so it means that the mesh is conformal in the junctions area (Figure 2).

Let us apply the forces $P = (p_1, p_2, \ldots, p_n)^T$ to the computational nodes, where p_i is the force applied to the node x_i. The determination of the displacements $U = (u_1, u_2, \ldots, u_n)^T$ in the computational nodes under these forces needs only solving the system of linear equations:

$$P = KU \tag{1.1}$$

where K is the flexibility matrix of the whole system.

Computational nodes are selected from finite element nodes located in the junction area. Computational net consists of nodes where displacements will be computed. Displacement values in other nodes of the junction area are calculated by the interpolation.

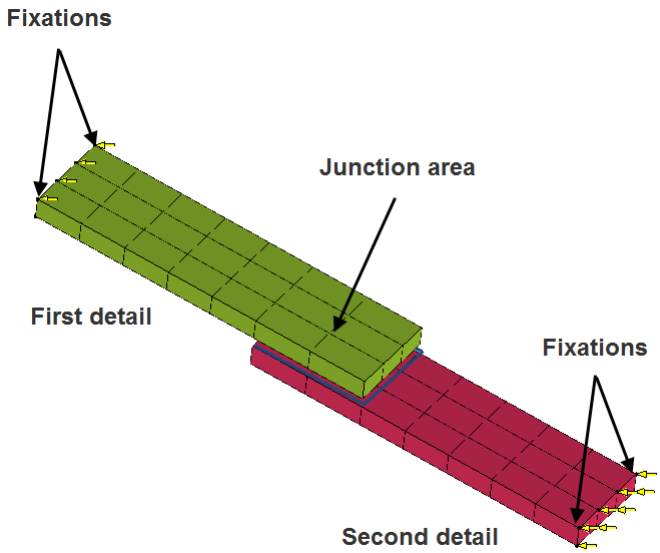

Figure 1: Finite element model

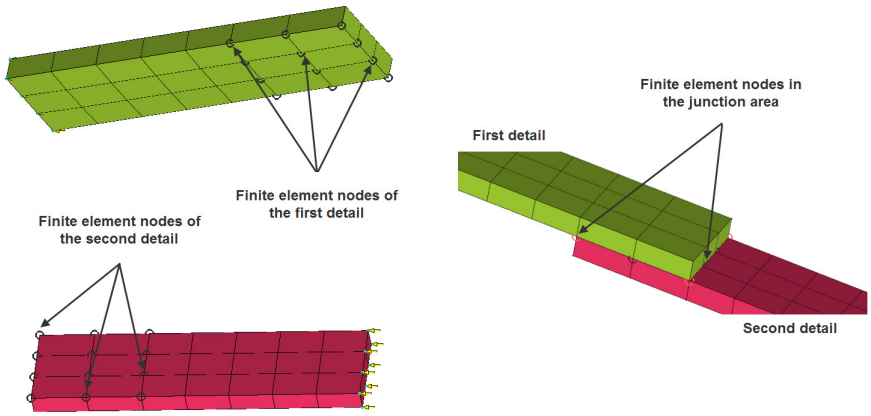

Figure 2: Finite element nodes in the junction area

In our model, only normal displacements of nodes is computed.

The main task of the algorithm is to compute the model's stiffness matrix. It can be calculated as Schur complement of stiffness matrix of each detail [4]. For this purpose, the flexibility matrix K of the model is constructed. It is calculated as the sum of flexibility matrices of each detail K_1 and K_2. To calculate the flexibility matrix of each detail, a unit force is applied to each node of the computational net. Displacements in each computational node caused by the applied force are calculated using the finite element method [1, 2, 6] and form the lines of this matrix. After that the stiffness matrix

is calculated by inversing the flexibility matrix of the model according to the equation:

$$R = K^{-1} \tag{1.2}$$

Further, the initial gap between computational nodes $D = (D_1, D_2, \ldots, D_n)$ and the forces applied to them $F = (F_1, F_2, \ldots, F_n)$ are set as it is shown in Figure 3.

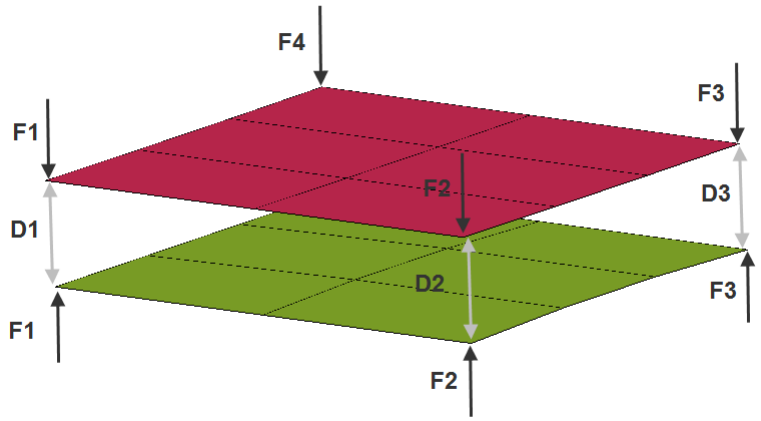

Figure 3: Initial gap and forces

To find the field of relative displacements of computational nodes under the influence of the loading set, the system potential energy minimization problem is solved under the given restrictions on displacements [5]. This means that if

$$W(U) = \frac{1}{2}U^T RU - F^T U \tag{1.3}$$

is the potential energy of system it is necessary to solve the following problem of optimization:

$$minW(U)\ on\ all\ U, so\ that\ U < D \tag{1.4}$$

The problem solution is the relative normal displacements of two details. The main goal of this paper is to solve the contact problem in the case of non-conformal meshes. Hereinafter, non-conformal meshes are meshes for which all or a part of finite element nodes in the junction area do not coincide. Otherwise, meshes are conformal. In this case, it is necessary to define which nodes to use as computational nodes and prepare the algorithm for the case of incoincident nodes.

2. Methodology

Consider the finite element model consisting of two details, fixed at the ends. The properties of each detail, such as the geometry, the material mechanical properties, the position of fixations, and the relative position of details are defined. Consider the case

when the finite element mesh of the first detail in the junction area differs from the finite element mesh of the second one as in Figure 4. It means, according to definition, that the finite element mesh in the junction area is non-conformal.

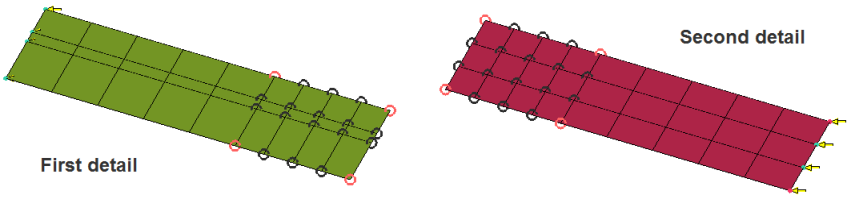

Figure 4: Finite element nodes in the junction area

Choose all finite element nodes of the first detail in the junction area as the computational nodes. Assuming that their number is less or equal to the number of finite element nodes of the second detail. Some finite element nodes of the second detail in the junction area coincide with computational nodes of the first detail and some do not.

The computing algorithm require that the computational nodes on both details should have identical space coordinates. Those nodes of the second detail for which exist corresponding computational nodes of the first detail called real. Points of the second detail corresponding to other computational nodes of the first detail called imaginary nodes. In Figure 5, the real nodes are marked in dark blue and the imaginary nodes are marked in yellow.

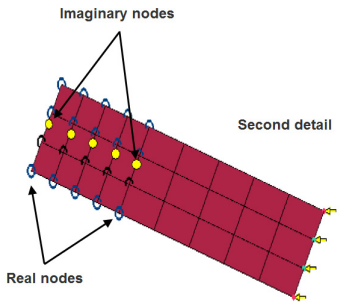

Figure 5: Computational nodes of the second detail

According to the main algorithm, the unit force is applied to all computational nodes of the first detail to obtain the first flexibility matrix. The same procedure should be done for the second detail. Now it needs to define how to interpret forces which should be applied to imaginary nodes and how to calculate displacements at these nodes. Two cases are possible:

1. The imaginary node is on the element border of the second detail.

2. The imaginary node is inside of the element.

Start with the case when the imaginary node is on the border of the element. Decompose the force F on two neighbor nodes, node 1 and node 2, so that the equations 5 and 6 are satisfied:

$$F_1 a_1 = F_2 a_2, \tag{2.1}$$

$$F_1 + F_2 = F, \tag{2.2}$$

where F_1, F_2 are forces, applied to the real neighbor nodes and a_1, a_2 are distances from imaginary node to the real neighbor nodes.

After that, displacements of the second detail under the influence of forces F_1, F_2 can be found. The displacements on the imaginary node is interpolated from real nodes using the following equation:

$$u_* = \frac{u_2 - u_1}{a_1 + a_2} a_1 + u_1, \tag{2.3}$$

where u_1, u_2 is displacements in the real nodes and u_* is the displacement in the imaginary node.

Consider now the case when the imaginary node is inside of the element. In this case, it is necessary to decompose the force on four real nodes 1, 2, 3, 4 of the element (Figure 6).

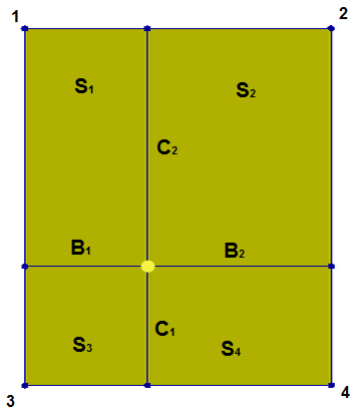

Figure 6: Force decomposition scheme when the imginary node is imside of the element

Find the force $F_k, k = 1, 2, 3, 4$ under the following equation:

$$F_k = a_k F, \tag{2.4}$$

where a_k is coefficients giving one in the sum:

$$a_1 + a_2 + a_3 + a_4 = 1. \tag{2.5}$$

It is possible to find coefficients a_k using the following scheme. Draw two straight lines through the imaginary node, perpendicular to the element sides. These straight

lines divide the element into four parts. Figure 6 shows the four parts of the element, where S_i, $i = 1, 2, 3, 4$ is the area of the each part.

Then coefficients a_k can be obtained using the following equations:

$$a_1 = \frac{S_4}{S}, a_2 = \frac{S_3}{S}, a_3 = \frac{S_2}{S}, a_4 = \frac{S_1}{S}, \tag{2.6}$$

where S is the area of the element. Check that the sum of the moments of all forces F_k in the imaginary node is equal to zero:

$$F_1c_2 + F_2c_2 = F_3c_1 + F_4c_1, \tag{2.7}$$

$$\begin{aligned} a_1Fc_2 + a_2Fc_2 - a_3Fc_1 - a_4Fc_1 &= \frac{F}{S}(S_4c_2 + S_3c_2 - S_2c_1 - S_1c_1) \\ &= \frac{F}{S}(c_1b_2c_2 + b_1c_1c_2 - c_2b_2c_1 - b_1c_2c_1) = 0, \end{aligned}$$

$$F_1b_1 + F_3b_1 = F_2b_2 + F_4b_2, \tag{2.8}$$

$$\begin{aligned} a_1Fb_1 + a_3Fb_1 - a_2Fb_2 - a_4Fb_2 &= \frac{F}{S}(S_4b_1 + S_2b_1 - S_3b_2 - S_1b_2) \\ &= \frac{F}{S}(c_1b_2b_1 + c_2b_2b_1 - b_1c_1b_2 - b_1c_2b_2) = 0, \end{aligned}$$

where b_1, b_2, c_1, c_2 are the distances from imaginary node to element borders. Deformation in the imaginary node is defined as sum of displacements in the real nodes of the element with coefficients a_k:

$$u_* = a_1u_1 + a_2u_2 + a_3u_3 + a_4u_4 \tag{2.9}$$

Finally, the general algorithm of software complex can be rewritten as:

Step 1. Unit force is applied to all computational nodes of the first detail. Corresponding deformations form the rows of the first flexibility matrix.

Step 2. Unit force is applied to all computational nodes of the second detail (to imaginary and to real nodes) and deformations under these forces are calculated. For the real computational nodes deformations are obtained directly, as it was for the first detail. For imaginary computational nodes the scheme of force decomposition and deformation interpolation, described above, is used. Thus, the flexibility matrix of the second detail is calculated.

Step 3. At the end, the first flexibility matrix should be added to the second flexibility matrix and the result matrix is the flexibility matrix of the whole system. The stiffness matrix is computed by inversing of the flexibility matrix.

Table 1: Initial data of the first detail for the first case.

Lx_1 (m)	Ly_1 (m)	E_1 (H/m^2)	Nu_1	S_1 (m)
1	2	10^7	0.3	0.01

Table 2: Initial data of the second detail for the first case.

Lx_2 (m)	Ly_2 (m)	E_2 (H/m^2)	Nu_2	S_2 (m)
1	2	10^7	0.3	0.01

3. Results

During this work, there has been considered a lot of cases with two membranes. In this article only two models is presented to show the results of modified algorithm for non-conformal meshes in the contact zone. Consider the first model of two membranes, shown in Figure 7.

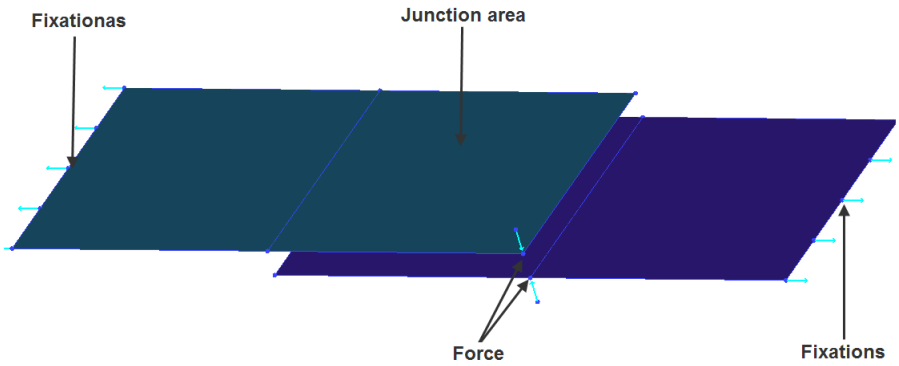

Figure 7: First example.

Initial data are presented in Tables 1-2.

Hereinafter, Lx_1, Lx_2 are lengths of details in the x direction, Ly_1, Ly_2 are lengths of membranes in the y direction, E_1, E_2 are Young's modules, Nu_1, Nu_2 are Poisson's ratios and S_1, S_2 are thicknesses of membranes. The initial gap $h = 0.01$ m is given. The force $F = 10$ H is applied to boundary nodes.

Firstly, consider the case when the decomposition of the first detail in the junction area is 8×8. Hereinafter, the first value is number of nodes in the x direction, the second one is number of nodes in the y direction. All these nodes will be used as computational nodes. Build the same mesh in the junction area for the second membrane, so the meshes are conformal now.

Figure 8 shows the deformation of the junction area in the case of conformal meshes. Initial positions of the junction area of plates are marked in red and dark blue, and deformed membranes are shown by yellow and blue.

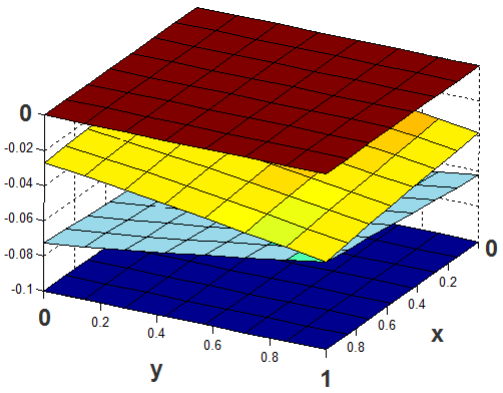

Figure 8: Solution of the first model in the case of the conformal mesh.

After that, increase the number of nodes in the contact area of the second membrane. The number of computational nodes is still 64. Let u_i be the deformation in ith node in case of conformal meshes, v_i is the deformation in ith node in case of non-conformal meshes and N the number of computational nodes. The relative error is denoted by:

$$E_{rel} = \frac{\sqrt{\sum_{i=1}^{N}(v_i - u_i)^2}}{hN} \tag{3.1}$$

It should be noticed that the stiffness matrix of the model is ill-conditioned. Interpolations can increase the condition number, that is presented by equation 15, and then the stiffness matrix can be either positive defined or not positive defined. Therefore, it needs to check the condition number because the stiffness matrix must be positive defined.

$$cond(R) = \frac{\lambda_{\max}}{\lambda_{\min}}, \tag{3.2}$$

where $\lambda_{\max}$ is the maximum eigenvalue of the stiffness matrix and λ_{min} is the minimum eigenvalue of the stiffness matrix. Therefore, the condition number of the stiffness matrix in case of non-conformal meshes is checked. The obtained results of the first case are presented in Table 3.

The dependence of the relative error on the total number of nodes in the junction area and the dependence of the condition number on the total number of nodes in the junction area are represented in Figure 9. The red line presents the condition number for the case with conformal meshes. The blue points show results of cases with non-conformal meshes.

Table 3: Results of the first case.

Decomposition of the junction area	Total number of finite element nodes	Condition number	Relative error
8×8	64	2.47E+05	0
9×9	81	4.62E+05	1.37E-05
10×10	100	4.10E+05	1.30E-05
12×12	144	3.81E+05	1.13E-05
14×14	196	3.61E+05	9.49E-06
17×17	289	3.31E+05	6.38E-06
19×19	361	3.21E+05	3.89E-06

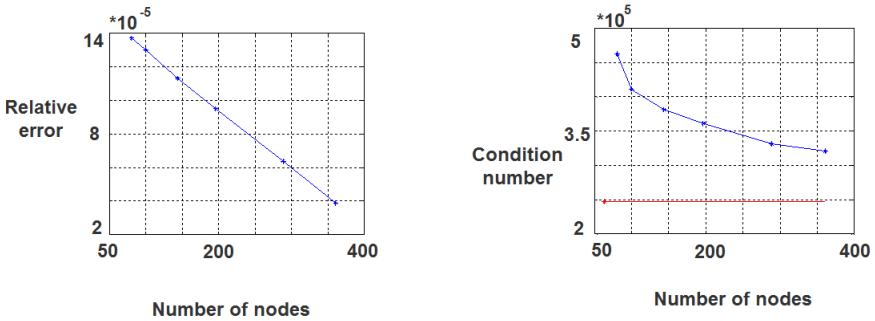

Figure 9: The dependence of the relative error on the total number of nodes in the junction area for the first example and the dependence of the condition number on the total number of nodes in the junction area for the first example.

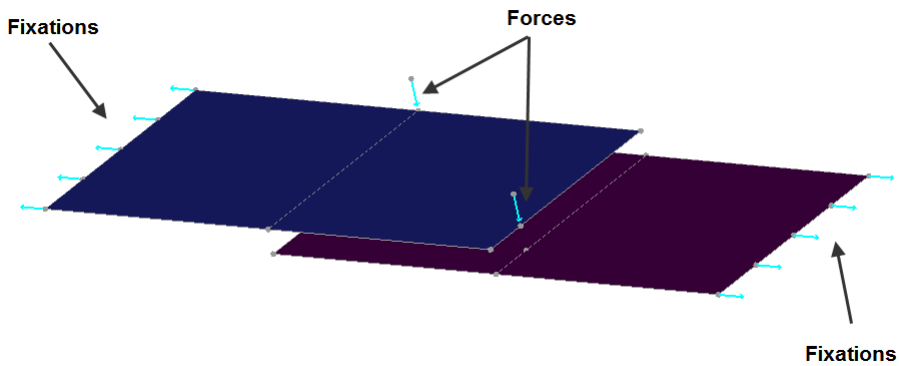

Figure 10: Second case.

Table 4: Initial data of the first detail for the second case.

Lx_1 (m)	Ly_1 (m)	E_1 (H/m^2)	Nu_1	S_1 (m)
1	2	10^{13}	0.2	0.005

Table 5: Initial data of the second detail for the second case.

Lx_2 (m)	Ly_2 (m)	E_2 (H/m^2)	Nu_2	S_2 (m)
1	2	10^{12}	0.3	0.01

Consider the second model consisting of two membranes, shown in Figure 10.

Tables 4-5 present the initial data for this case.

The initial gap h is 0.01 m. The force $F = 10^5$ H is applied to nodes as it is shown in Figure 10.

Let here the decomposition of the first plate in the contact zone is 5×11. As for the first case, all these nodes are taken as the computational nodes. Repeat the same algorithm that is the same for the previous case. The solution of the contact problem with conformal meshes is shown in Figure 11.

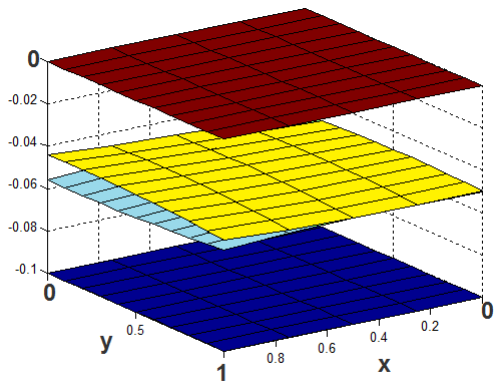

Figure 11: Solution of the contact problem for the second case.

Obtained results for non-conformal meshes are presented in Table 6 and in Figure 12.

4. Conclusion

During this work the method for using of non-conformal meshes in the contact problem decision for airframe assembly simulation has been developed. In the case of membranes, the maximum relative error does not exceed 1% and the condition number increases by

Table 6: Results for non-conformal meshes in the second case.

Decomposition of the junction area	Total number of finite element nodes	Condition number	Relative error
5×11	55	6.68E+05	0
8×8	64	1.12E+06	8.02E-05
8×17	136	8.81E+05	6.52E-05
8×23	184	7.99E+05	6.39E-05
8×32	256	7.67E+05	6.32E-05
8×39	312	7.29E+05	6.29E-05
8×45	360	7.20E+05	6.28E-05

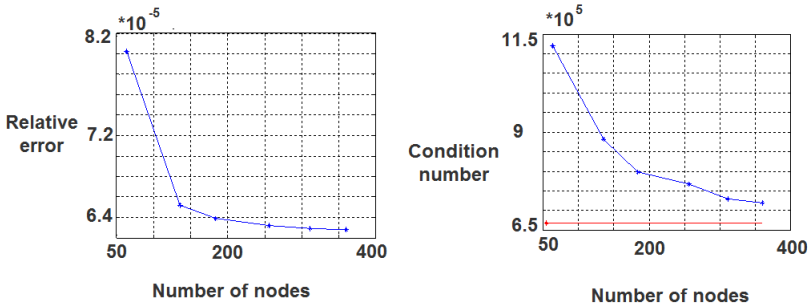

Figure 12: The dependence of the relative error on the total number of nodes in the junction area for the first example and the dependence of the condition number on the total number of nodes in the junction area for the first example.

no more than 1.5 times. Therefore, the given algorithm can be used in practice. Also it should be noticed that for the considered cases using of non-conformal meshes does not increase the time of calculations.

References

[1] Bathe K.J., Wilson E. L., 1976, "Numerical Methods in Finite Element Analysis", Prentice-Hall Inc.

[2] Clough R. W., 1960, "The finite element method in plane stress analysis", Proc. American Society of Civil Engineers (2nd Conference on Electronic Computation, Pitsburg, Pennsylvania), Vol. 23, P. 345–378.

[3] Lupuleac S., Petukhova M., Shinder Y., Bretagnol B., 2011, "Methodology for

Solving Contact Problem during Riveting Process", SAE International Journal of Aerospace, 4(2), 952–957.

[4] Lupuleac S., Shinder Y., Petukhova M., Yakunin S., Smirnov A., Bondarenko D., 2013, "Development of Numerical Methods for Simulation of Airframe Assembly Process", SAE International Journal of Aerospace, 6(1):101–105, doi:10.4271/2013-01-2093.

[5] Petukhova M., Lupuleac S., Shinder Y., Smirnov A., Yakunin S., Bretagnol B., 2014, "Numerical approach for airframe assembly simulation", Journal of Mathematics in Industry, 4:8.

[6] Sigerlind L. J., 1976, "Applied Finite Element Analysis", John Wiley and Sons Inc.